COMPUTATIONS FOR LAMINAR FLOW CONTROL IN SWEPT-WING BOUNDARY LAYERS

Helen L. Reed*, Richard G. Rhodes*, William S. Saric*
***Texas A&M University**

Keywords: *stability, transition, crossflow, control, computations*

Abstract

The laminarization of a swept-wing boundary layer by the introduction of passive spanwise-periodic discrete roughness elements (DREs) near the leading edge is modeled by linear stability theory without curvature (LST) and nonlinear parabolized stability equations (NPSE). Studies predict that, for chord Reynolds numbers of 8 million and with an appropriate pressure coefficient design, the crossflow instability can be stabilized and laminar flow achieved. Sensitivity to element placement and height is studied, and it is shown that the optimum location for the control elements is at the Branch I neutral point of the control wavelength. This work serves as a companion to flights tests of a swept-wing model mounted below the wing of a Cessna O-2 aircraft at Texas A&M's Flight Research Laboratory.

1 Introduction

Transition to turbulence and laminar flow control (LFC) in flight have received considerable attention over the past seven decades or so (Green 2008). In low-disturbance environments such as flight, boundary-layer transition to turbulence generally occurs through the uninterrupted growth of linear instabilities. The initial conditions for these instabilities are introduced through the receptivity process, which depends on a variety of factors (Saric et al. 2002). Because transition location can be a significant source of uncertainty in the accurate prediction of aerodynamic forces (lift and drag) and heating requirements, research in the area of boundary layer stability and transition has been quite vigorous. Comprehensive reviews for both 2-D and 3-D flows are given by Mack (1984), Reed & Saric (1989, 2008), Arnal (1994), Reshotko (1994), Saric (1994), Reed et al. (1996), Saric et al. (2003), and the recent RTO course "Advances in Laminar-Turbulent Transition Modeling", 9-12 June 2008, by Saric, Reshotko, Arnal, & Reed, taught at VKI.

Four basic instability mechanisms generally contribute to transition on a swept aircraft wing.

- Leading-edge radius and sweep give rise to attachment-line contamination and instability (Pfenninger 1965, 1977, Cumpsty & Head 1967, Gaster 1967, Pfenninger & Bacon 1969, Poll 1979, 1985, Hall et al. 1984, Reed & Saric 1989, Saric et al. 2003, Arnal 2008, Reed 2008) but this can be controlled by keeping the leading-edge radius below a critical value, or eliminating contamination from the wing root through suction or a Gaster bump..
- Streamwise instabilities related to the Tollmien-Schlichting (T-S) mechanism typically occur in the mid-chord region and transition can be reasonably correlated (Mack 1984, Reed et al. 1996, Arnal 2008). The T-S instability can be effectively controlled by (1) weak favorable pressure gradients, (2) weak wall suction, or (3) wall cooling. The last two items represent some additional mechanical complications. It is now well known that using a favorable pressure gradient and minimizing the extent of the pressure-recovery region both contribute to the control of this instability. The T-S instability is more

strongly influenced by freestream sound than by freestream turbulence within some limits on freestream turbulence. Freestream turbulence is not a dominant feature of flight conditions. The T-S instability is more strongly influenced by 2-D roughness than 3-D roughness within some limits on 3-D roughness. If the flow is not accelerated, steps and gaps can trip the boundary layer.

- The crossflow instability has been the primary challenge holding back LFC. Favorable pressure gradients used to stabilize streamwise instabilities destabilize crossflow. For years, it seemed as though the only solution to crossflow control was surface suction. The perceived complications with moving parts and additional maintenance were always discouraging factors toward laminarizing swept wings. This final hurdle may have been overcome with passive nonlinear biasing of stationary crossflow wave growth (Saric et al. 1998). This is the subject of this paper.
- Concave curvature can give rise to Görtler instabilities (Saric 1994) but this can be controlled by the appropriate profile design. Saric & Benmalek (1991) show that convex curvature has an extraordinary stabilizing influence on the Görtler vortex, and they give examples of wavy-wall computations where the net result is stabilizing. As a potential application, supercritical airfoils for high subsonic transports have been designed with sharp leading edges requiring a series of corners or a concave surface to provide section thickness downstream (Pfenninger et al. 1980).

There are additional factors which affect swept-wing transition.

- Wing/fuselage and /pylon junctures, and similar configurations are classified as 3-D corner flows, exhibit crossflow characteristics, and can contaminate neighboring laminar flow regions.
- The effect of compressibility in the high subsonic/low supersonic range is normally stabilizing, and at supersonic speeds the nature of the instabilities changes. As a potential application, transport aircraft can locally achieve low supersonic Mach numbers on the suction side of the wing and linear stability analysis uncovers that the most unstable disturbances are 3-D and driven by a generalized inflection-point in the boundary layer. For higher supersonic Mach numbers, an acoustic mode (second mode) dominates (Mack 1984).
- Surface features such as bumps, steps, gaps, and surface waviness, affect transition based on their geometry, size, and location. Due to the nature of the instabilities, (within limits) T-S is destabilized by 2-D features, and crossflow and Görtler by 3-D features.

The efficacy of transition control depends largely on the physics of the transition process. Whether one desires to delay transition by the various techniques of LFC (Pfenninger, 1965, 1977; Reshotko, 1984, 1985; Collier 1993; Joslin 1998; Arnal 2008) or to encourage transition for enhanced mixing or separation delay, the most effective strategy is to capitalize on the most unstable disturbances. Knowledge of the transition process is key to efficient application.

2 Crossflow Instability

For aircraft with swept wings, the crossflow instability occurs in the regions of strong pressure gradient, primarily near the attachment line. In the inviscid region outside the boundary layer, the combined influences of sweep and pressure gradient produce curved streamlines at the boundary-layer edge. Inside the boundary layer, the streamwise velocity is reduced but the pressure gradient is unchanged. Thus, the balance between centripetal acceleration and pressure gradient does not exist. This imbalance results in a secondary flow in the boundary layer called crossflow that is perpendicular to the direction of the inviscid streamline. The 3-D profile and resolved streamwise and crossflow boundary-layer profiles are shown in Figure 1.

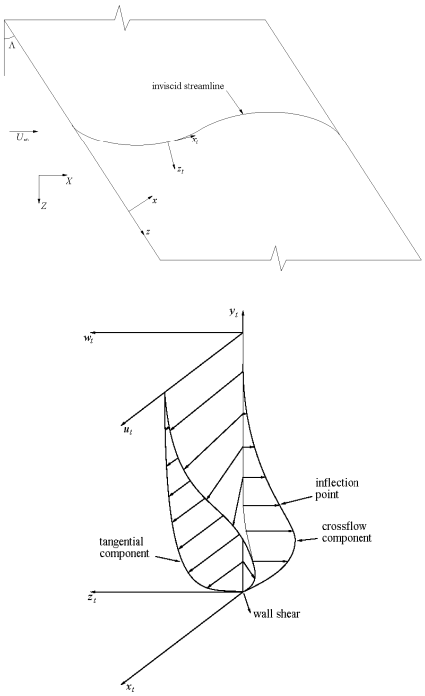

Fig. 1. Flow over a swept wing and the resolved local streamwise and crossflow boundary-layer profiles. Note the inflection point in the crossflow profile.

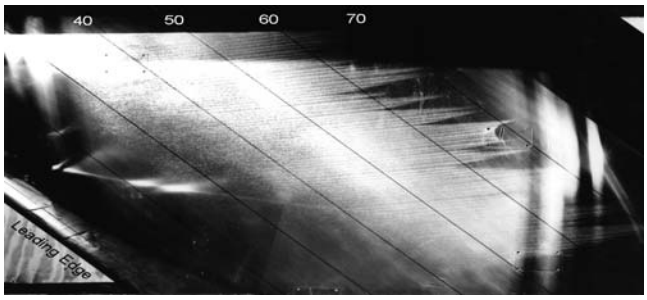

Fig. 2. Flow over a swept wing in a quiet wind tunnel showing the stationary pattern of the crossflow instability characteristic of flight. From Radeztsky et al. (1993).

Because the crossflow velocity must vanish at the wall and at the boundary-layer edge, an inflection point exists and provides a source of an inviscid instability mechanism. Unlike T-S instabilities, the crossflow problem exhibits stationary as well as traveling disturbances that are amplified. Even though both types of waves are present in typical swept-wing or rotating-disk flows, transition is usually caused by either the stationary or the traveling waves. Although linear theory predicts that the traveling disturbances have higher growth rates, transition in many experiments is induced by stationary waves. Whether stationary or traveling waves dominate is related to the receptivity process. Stationary waves are more important in low-turbulence environments characteristic of flight, while traveling waves dominate in high-turbulence environments (Bippes 1997; Deyhle & Bippes 1996). In the flight environment, the presence of micron-sized 3-D roughness at the leading edge (e.g. from a painted surface) establishes the stationary streamwise vortex. In fact, the 3-D boundary layer is ultra sensitive to this roughness, yet this roughness has no effect on streamwise disturbances (Radeztsky et al., 1993). In interacting with inherent surface roughness, freestream turbulence appears to be the source of travelling crossflow, but freestream turbulence is not a dominant feature of flight conditions (White & Saric 2005). Therefore, in flight, the instability appears as stationary co-rotating vortices whose axes are aligned to within a few degrees of the local inviscid streamlines. The wavelength of these vortices is approximately four times the local boundary-layer thickness. See Figure 2.

Stationary crossflow waves (v' and w' disturbances) are typically very weak, hence analytical models have been based on linear theory. However, experiments often show evidence of strong nonlinear effects (Dagenhart et al 1989, 1990; Bippes & Nitschke-Kowsky 1990; Bippes et al 1991; Deyhle et al 1993; Reibert et al 1996). Since the wave fronts are fixed with respect to the model and nearly aligned with the potential-flow direction (i.e., the wavenumber vector is nearly perpendicular to the local inviscid streamline), the weak (v', w') motion of the wave convects $O(1)$ streamwise momentum producing a strong u' distortion in the streamwise boundary-layer profile. This integrated effect and the resulting local distortion of the mean boundary layer leads to the modification of the basic state and the early development of nonlinear effects. See also Haynes & Reed (2000) and Figure 3.

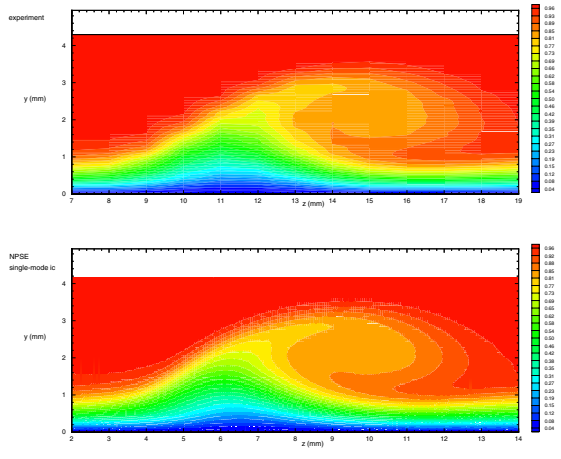

Fig. 3. Streamwise-velocity contours for a swept wing showing the nonlinear distortion due to the stationary crossflow vortex pattern typical of flight. Example of successful validation: Top figure – experiments of Reibert et al. 1996; lower figure – NPSE computations of Haynes & Reed (2000).

An interesting feature of the stationary crossflow waves is the destabilization of secondary instabilities. The u' distortions created by the stationary wave are time-independent, resulting in a spanwise modulation of the mean streamwise velocity profile. As the distortions grow, the boundary layer develops an alternating pattern of accelerated, decelerated, and doubly inflected profiles. The inflected profiles are inviscidly unstable and, as such, are subject to a high-frequency secondary instability. This secondary instability is highly amplified and leads to rapid local breakdown. Because transition develops locally, the transition front is nonuniform in span and characterized by a "saw-tooth" pattern of turbulent wedges See Kohama et al (1991, 1996), Kawakami et al. (1999), Malik et al. (1994, 1996, 1999), Janke & Balakumar (2000), Wasserman & Kloker (2002), and White & Saric (2005).

What is known is that in flight, the crossflow instability is stationary. Because the crossflow instability is driven by an inflection point away from the wall, suction and wall cooling are much less effective than for T-S waves and consequently stronger levels need to be applied for control. Crossflow is destabilized by both favorable and adverse pressure gradients. Also, opposite to 2-D T-S waves, the 3-D crossflow instability is more strongly influenced by freestream turbulence than by freestream sound. Also, opposite to 2-D T-S waves, the crossflow instability is ultra-sensitive to micron-sized 3-D roughness, but not 2-D roughness. Stationary crossflow wave growth is also extremely sensitive to very weak convex curvature.

What is especially exciting is that Saric et al. (1998) are able to capitalize on the physics associated with the mean-flow distortion created by the stationary vortices and suggest a passive control scheme through the application of spanwise-periodic roughness near the leading edge for LFC (DREs, spanwise-periodic discrete roughness elements). This offers a possible alternative to the use of suction to control crossflow on transports.

3 Discovery of DRE Control

Surface roughness is the important crossflow receptivity mechanism in flight. Three configurations have been investigated experimentally in the Klebanoff-Saric Unsteady Quiet Wind Tunnel[1] in a low-disturbance freestream environment and stationary-wave-dominated boundary layer. The model is an NLF(2)-0415 airfoil swept 45º and features a favorable pressure gradient back to 71% chord to stabilize streamwise instabilities and destabilize crossflow. A small-radius leading edge meant no attachment-line instability or contamination and no concave curvature in the transition region meant no Görtler vortices. An infinite span was simulated to facilitate validation with the computations – to this end, there was no taper, and root and tip wall liners were applied in the tunnel.

To systematically study the effects of roughness, the surface was first highly polished to ≈0.2 microns. The most unstable *stationary* mode was determined from LST to be 12 mm (*parallel to the leading edge* and corresponding to a crossflow wavelength ≈4δ); this was

[1] Recently moved to Aerospace Engineering, Texas A&M

confirmed by the experiment – the 12 mm disturbance was found to dominate and cause transition. For random, natural-surface roughness, transition improvements were obtained by decreasing the rms roughness level from 3.3 μm to 0.2 μm. For chord Reynolds number $Re_c = 2.4 \cdot 10^6$, this roughness decrease delayed transition from 45% to 65% chord.

When discrete roughness ≈6 μm high (which corresponds to a roughness Reynolds number of $Re_k \approx 0.1$[2]) at 12 mm spanwise-periodic spacing was applied at approximately 2% chord near the leading edge (which corresponds to the neutral stability point for the 12 mm disturbance), the flow downstream became highly organized. Transition moved forward to 45% chord.

Saric et al. (1998) then systematically applied micron-sized roughness of different spanwise spacings near the leading edge to cause different crossflow disturbances to dominate downstream. They observed that unstable waves occur downstream only at integer multiples of the primary disturbance introduced by the roughness and no subharmonic disturbances are destabilized. That is, a roughness spacing at the leading edge of 12 mm (in the spanwise direction) produced crossflow disturbances downstream of 12, 6, 4, … mm wavelengths. The following table summarizes the results:

LE roughness spacing (mm)	Crossflow wavelengths observed downstream (mm)
12	12, 6, 4, …
36	36, 18, 12, 9, 7.2, 6, 5.1, …
18	18, 9, 6, …
8	8, 4,…

Roughness height [μm] / spacing [mm]	x/c of transition
0.2 / random	65%
6··· 50 / 12	45%
6 / 36	45%
6 / 8	>80% laminar wing

Note that forcing at 18 and 8 mm inhibits the appearance of the most unstable disturbance of 12 mm. Moreover, subcritical forcing at 8 mm spanwise spacing actually delays transition beyond the pressure minimum and onto the trailing-edge flap (>80% chord). See Figures 4 and 5. By itself, the 8 mm mode does not lead to transition, but during the rapid growth of this mode, the *mean flow* is changed and the 12 mm mode and higher wavelengths are suppressed, thus delaying transition. The 8 mm disturbance decays without tripping the flow and laminar flow is maintained on the wing. Subcritical forcing at 8 mm spanwise spacing *actually delays transition beyond that of the highly polished condition (0.2 μm), beyond the pressure minimum, and well beyond 80% chord* (the actual location was beyond view). Figures 4 and 5 show crossflow-vortex visualization via naphthalene applied to the airfoil surface for the Saric experiment. Figure 4 is the case with no control – natural transition is at 65% chord. Figure 5 is the case with discrete roughness of subcritical 8-mm spanwise-periodic spacing applied at the leading edge – laminar flow beyond 80%.

Saric et al. (1998) also noted that the artificial spanwise-periodic discrete roughness has no effect if not applied within the first 2%-5% chord. Also, it was demonstrated that this idea works on a standard aircraft finish surface. Saric et al. (2000) applied paint to the wing; this provided a background random roughness with peak to peak roughness between 11 and 30 microns. They then biased this background roughness with 50 micron roughness (which corresponds to a roughness Reynolds number of $Re_k \approx 7$) at 8 mm spacing applied at the leading edge (as above). With no control, transition was observed to occur at 40% chord. With discrete roughness at the subcritical spanwise-periodic spacing of 8 mm, again transition was delayed until well past the pressure minimum and onto the flap (>80% chord).

Saric and co-workers also showed that holes and glow discharge work equally as well as bumps, and that bump shape is not important just the spacing and height. This can be accomplished by spanwise-periodic discrete roughness, holes, or glow discharge. Providing

[2] The Braslow criteria suggests that the flow will not trip for roughness Reynolds number below 150 (.von Doenhoff and Braslow, 1961).

the initial 3-D biasing to the flow is the key. These experiments show that transition control is possible using a passive roughness distribution near the attachment line.

Subsequent to the Saric experiments, the NPSE results (Haynes & Reed 2000) and a DNS solution, Wassermann & Kloker (2002) confirmed this effect.

This promising technique was also begun to be demonstrated for supersonic flight (Saric & Reed 2002).

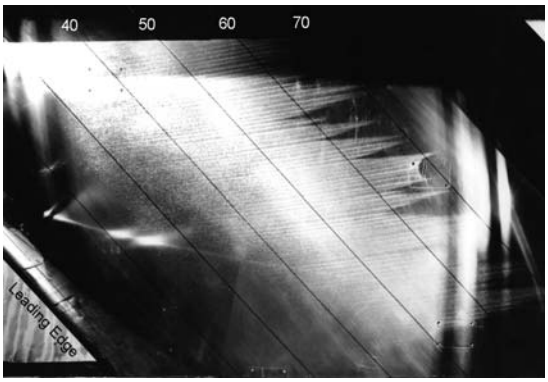

Fig. 4. Natural transition at 65% chord.

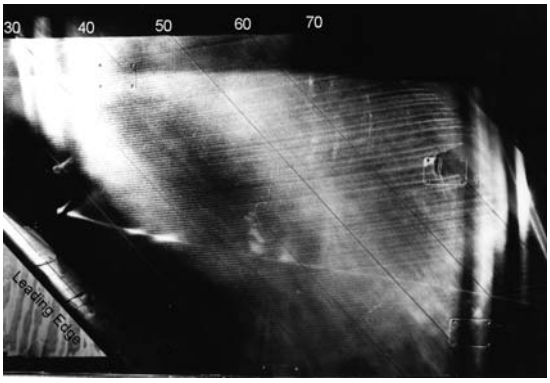

Fig. 5. DRE control of 8-mm spacing at leading edge. Transition delayed beyond 80% chord.

4 DRE Control Design Strategy

According to Saric & Reed (2002, 2003), the main ideas to consider during the design of the airfoil are to encourage crossflow, eliminate streamwise and attachment-line instabilities, and allow shorter wavelengths to grow sufficiently, early enough for control of the most unstable wavelength. The initial part of the design procedure is to have an accelerated flow that is subcritical to streamwise instabilities (T-S waves). When considering natural or passive LFC under flight Reynolds numbers of 50 million or so, it is injudicious to work at the margins of this instability. The present design philosophy is to eliminate streamwise instabilities and concentrate on meanflow modifications to reduce the growth of crossflow waves.

To implement spanwise-periodic discrete roughness (or holes or glow discharge) for laminar flow control, one recognizes that in the flight environment, stationary crossflow is the dominant instability. One first identifies the most unstable stationary crossflow wavelength, λ_{crit} (again, it is easiest to reference this length as being parallel to the leading edge). Linear stability theory (without curvature) assuming stationary disturbances accurately predicts this critical wavelength and the location at which it first becomes unstable (neutral point). The neutral point of the critical wavelength is the placement location for the DREs. Then one studies stationary crossflow of shorter, *subcritical* wavelengths, λ_{sub}. These are the waves we will force by roughness for control. Therefore it is necessary that these waves grow strongly earlier than the critical wave, but then decay downstream after $O(40\%)$ chord. The observation is that the C_p distribution can be so designed that waves of about half the wavelength of the most unstable wave will grow sufficiently and then decay, thus changing the basic state and not allowing the most unstable wave to take hold. One must be cautious in C_p design that the stability N-factors do not become too large.

Therefore, an airfoil conducive to LFC by DREs must feature uniformly accelerated flow so that T-S waves are stable. With wing sweep, this favorable pressure gradient will be very unstable to crossflow. The associated C_p distribution must allow shorter-wavelength disturbances to grow sufficiently in the leading-edge region to nonlinearly modify the basic state and inhibit the growth of the longer-wavelength most-unstable disturbance. Thus transition will be delayed.

Note in general that DRE control cannot be retrofitted to any wing. The C_p distribution must be designed to be conducive to the DRE strategy. Nor will a C_p distribution designed for lower chord Reynolds number necessarily work for higher chord Reynolds number. A new C_p distribution must be generated for the new operating conditions.

5 Present Work: Application to Higher Chord ReynoldsNumbers

The Saric experiments were conducted at a nominal chord Reynolds number of 2.4 million. The next objective was to demonstrate the technology at higher chord Reynolds numbers of 7-8 million applicable to high-altitude, long-duration unmanned aerial vehicles (UAVs). As noted above, the crossflow instability has been well documented to be hyper sensitive to both micron-sized roughness and freestream vorticity. It was found that freestream vorticity inherent in wind tunnels operating at these flight Reynolds numbers and Mach numbers induced travelling crossflow. Even the best tunnels are challenged when the Mach number exceeds 0.25. In flight, this small-scale turbulence is absent, making flight testing the only possibility for careful research in this area.

The Cessna O-2 Skymaster is a top-wing aircraft with a twin-boom tail and both a pusher and a tractor propeller used by the Texas A&M Flight Research Lab (FRL) to conduct flight research. The O-2 is well suited for flight research as it has mounting points at roughly half span of both the port and starboard wings which can accommodate a wide range of test equipment and models. The current study focuses on the spanwise-periodic DREs to maintain laminar flow on a 30° swept wing test article (SWIFT) flown underneath the port wing of the aircraft. The SWIFT model has a 4.8 meter chord and 3.66 meter span, and is operated at chord Reynolds numbers between 7.5 million and 8 million. Two rows of streamwise pressure ports were built into the SWIFT on the suction side located at the 1/3 and 2/3 spanwise stations. Transition location is visualized via infrared thermogaphy. Careful attention is paid to well-defined and controlled operating conditions and surface roughness levels and detailed freestream disturbance levels. See Saric et al. (2008) and Figure 6.

Fig. 6. O-2 Skymaster with the SWIFT model attached beneath the port wing.

After the successes and lessons learned with the Saric experiments, the SWIFT model was initially specially designed for DRE control with LST (*without curvature*) assuming *stationary* crossflow. Here the airfoil shape was designed to feature favorable pressure gradients to inhibit the growth of streamwise instabilities (T-S waves), and be such that subcritical disturbances grow sufficiently to modify the basic state and inhibit the growth of critical disturbances.

In order to avoid prematurely tripping the boundary layer, particular attention was paid to both attachment-line contamination. As far as the former is concerned, the attachment-line momentum-thickness Reynolds number $Re_{\vartheta \mathrm{AL}}$ is kept below 100 so that disturbances cannot propagate along the attachment line, feeding into the boundary layer (according to Pfenninger (1977) and Poll (1985)). In other words,

$$Re_{\theta \mathrm{AL}} = 0.404\left[Re' r \tan\Lambda \sin\Lambda /(1+e)\right]^{1/2} \le 100$$

where *Re´* is the unit Reynolds number, *r* is the leading-edge radius in the direction *normal to the leading edge*, Λ is the leading edge sweep angle, and *e* is the ellipticity of the leading edge.

LST without curvature serves to predict the most unstable wavelengths and very early growth, but does not capture the physics of the breakdown process. Here it is necessary to apply the nonlinear parabolized stability equations (NPSE; Herbert 1997), which have become a popular approach to stability analysis owing to their inclusion of nonparallel, curvature, and nonlinear effects with relatively small additional resource requirements as compared with direct numerical simulations, or DNS. Moreover NPSE has been demonstrated to accurately model the transition process for a wide variety of convective flows, including crossflow, when the environment and operating conditions are modeled correctly. See Reed (2008).

In addition a highly accurate basic state is required for the stability calculations, so that a complete-aircraft CFD meanflow analysis is conducted hand-in-hand with the flight tests. The local flow-field around the test article must be very accurately modeled and well resolved. The results of this study will also help validate the flight test configuration and operating conditions. Physical limitations restrict the placement of data probes during flight, therefore CFD analysis is needed to quantify the influence the airplane has on the SWIFT.

5.1 CFD Meanflow Calculations

To model the meanflow, a simplified solid model of the O-2 and accompanying SWIFT model was created using Solidworks™. It was determined that the tail assembly, starboard boom, and starboard strut were located far enough away from the area of interest to have any influence and were thus discarded from the simulation. The region under the port wing (including the SWIFT model and its mount) was completely reconstructed using measurements taken directly from the aircraft. See Figure 7. The resulting solid model was then imported into GAMBIT™, which was used to create a computational mesh around the O-2. The CFD solver FLUENT™ was then used to generate the flow solutions for this mesh.

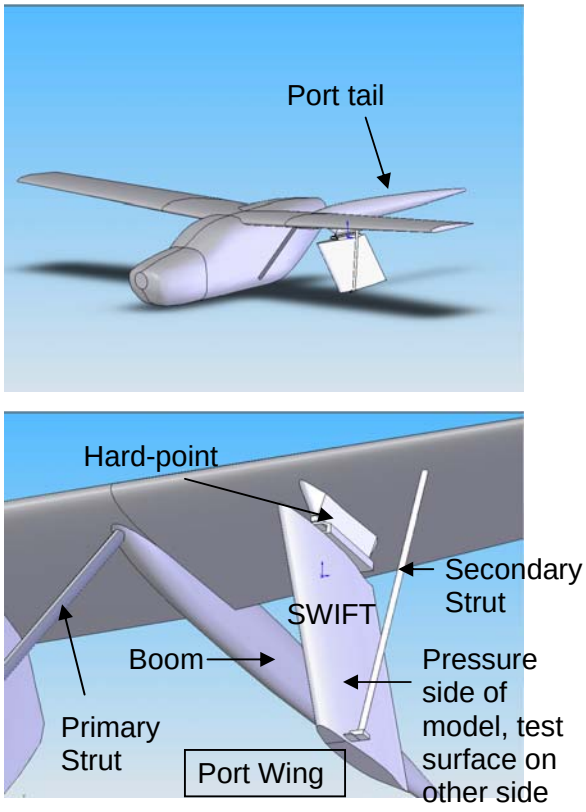

Fig. 7. CFD modeling of the O-2 and the SWIFT model

A grid convergence study was conducted starting with a fully unstructured tetrahedral grid using an inviscid solver. This allowed the minimum computational domain limits to be found. Refinement of the unstructured mesh near the SWIFT yielded a converged mesh for the inviscid solution based on the pressure distribution over the two rows of pressure ports mounted on the suction side of the SWIFT. To accurately model the boundary layer over the SWIFT using an unstructured mesh required a cell count significantly larger than what the computational resources could handle. This limitation dictated that a hybrid approach be taken. To gain the desired boundary layer fidelity a structured mesh was wrapped around the SWIFT. This structured region was then embedded in a larger unstructured mesh and connected using grid interfaces. This hybrid approach allowed grid convergence for a viscous laminar solution. See Figure 8.

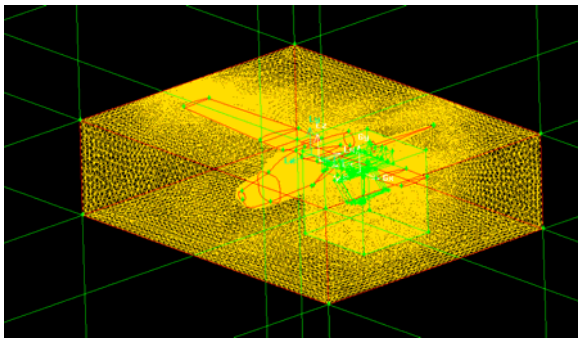

Fig. 8. Gridding of the O-2 and SWIFT model

In addition to grid convergence, a parametric study was conducted to determine the effects of both the propeller, and the small safety strut attached to the non-test side of the SWIFT model. The propeller was modeled by embedding a rotating propeller in the computational mesh of the O-2. See Figure 9. This propeller mesh was connected to the rest of the mesh by means of a grid interface, which allowed the propeller to "spin" requiring an unsteady solution. The small safety strut attached to the pressure side of the SWIFT has the cross-section of a symmetric airfoil and thus has an associated wake depending on its angle of attack with the freestream which could affect the flow over the SWIFT. To determine if the strut's angle of attack could affect the flow over the SWIFT, meshes were created with the strut rotated with an angle of attack ±20°. Neither of these studies showed any significant affect on the pressure distribution on the suction side of the SWIFT, thus the unsteady solution with the propeller was abandoned, and no more attention was paid to the angle of attack of the strut. See Figures 10 and 11.

Once a robust solution had been obtained, a study was conducted to determine the bowing affect that the fuselage had on the flow over the SWIFT and how this needs to be factored in to a comparison between flight test and the CFD solution. Because the flight conditions are recorded on the starboard wing and the SWIFT model is mounted on the port wing any bowing of the flow around the fuselage would introduce error in the angle of attack recorded for the SWIFT. The flowfield obtained from the CFD solution indeed showed significant bowing of the flow around the fuselage and a discrepancy in sideslip angle between the port and starboard mounting points. See Figure 12. This analysis was used to derive corrections to apply to recorded flight conditions and was also used to determine a better location for mounting the freestream probe. The resulting comparison between flight and CFD Cp distributions is excellent. The error bars on the flight data are ±0.0005 Cp. See Figure 13.

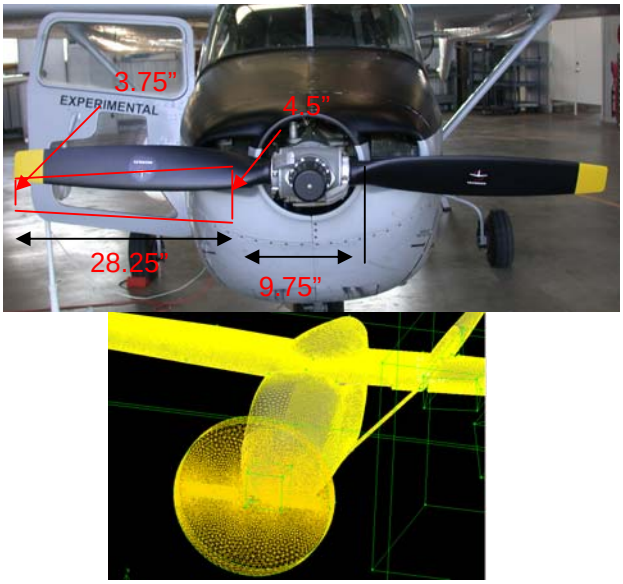

Fig. 9. Modelling the propeller.

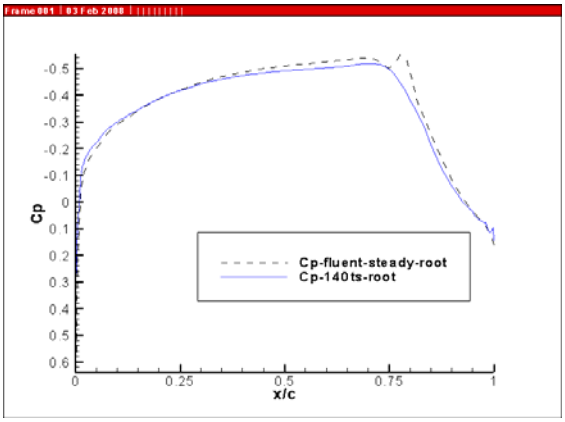

Fig. 10. Converged unsteady (propeller) pressure coefficient curve vs. steady solution without propeller. Conclude that the propeller has negligible effect on the SWIFT model.

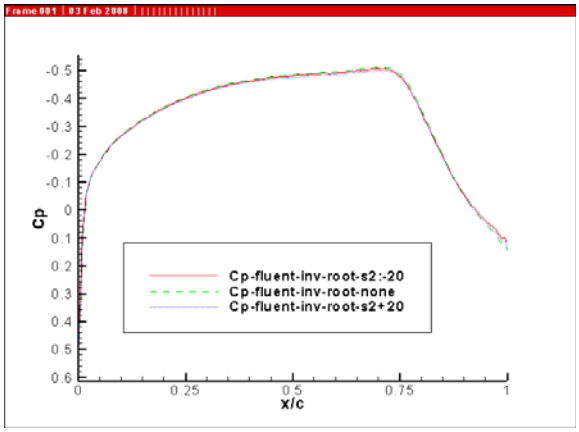

Fig. 11. Pressure coefficient curve on suction side of SWIFT for strut at +/- 20 deg AOA. Conclude that the strut has negligible effect on the suction side (test side) of the SWIFT model.

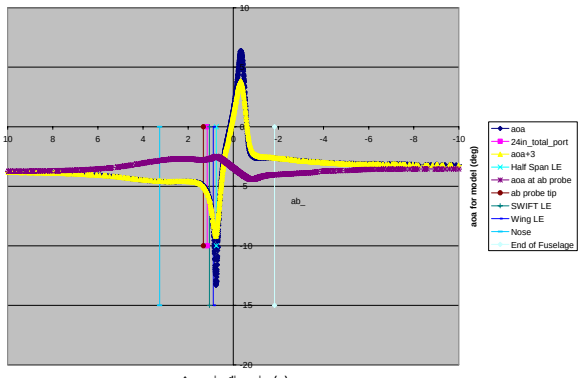

Fig. 12. CFD prediction of flowfield sideslip angle measured at port wing and starboard wing

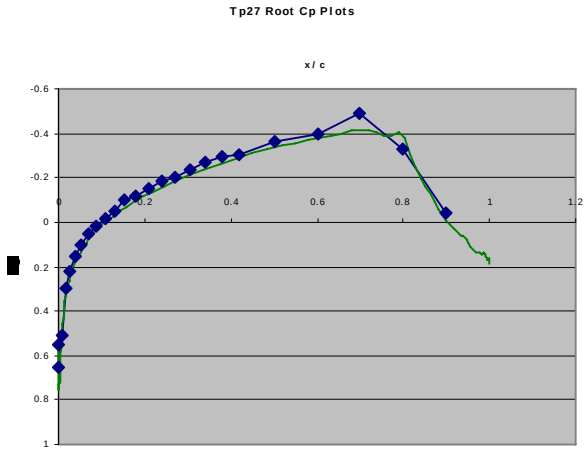

Fig. 13. Good agreement between flight (symbols) and CFD: -Cp curve on suction side. Representative at 33% span on SWIFT model.

5.2 Stability Calculations

With a validated boundary-layer profile over the suction side of the SWIFT, the next step is to perform a stability analysis to determine the nonlinear evolution of unstable disturbance modes of the boundary layer. The modeling of the introduction of the passive spanwise-periodic roughness elements (DREs) near the leading edge is underway through the application of both LST and NPSE. Calculations thus far suggest the feasibility of 2-mm spanwise-periodic spaced roughness elements to control natural crossflow with a 4-mm wavelength (Figure 14).

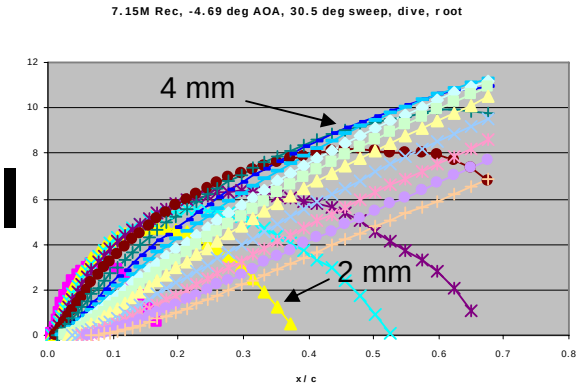

Fig. 14. LST for the SWIFT model shows the crossflow instability wavelength predicted in the range of 4 mm. DREs spaced 2 mm apart at the leading edge will control the crossflow. Wavelengths of the same order (e.g 2.25 mm) have the same effect.

Nonlinear studies completed thus far suggest that, for chord Reynolds numbers of 7-8 million and with an appropriate pressure coefficient design, the crossflow instability can be stabilized and laminar flow achieved. Sensitivity to element placement and height is predicted, and it is shown that the optimum location for the control elements is at the Branch I neutral point of the control wavelength. Comparisons with flight test results are forthcoming.

References

[1] Arnal D. 1994 Predictions based on linear theory. AGARD Rpt 793. Special Course on Progress in Transition Modelling

[2] Arnal, D. 2008 RTO course “Advances in Laminar-Turbulent Transition Modeling”, 9-12 June 2008, VKI, Brussels.

[3] Bippes H, Nitschke-Kowsky P. 1990 Experimental study of instability modes in a three-dimensional boundary layer. AIAA J. 28(10):1758-63

[4] Bippes H, Müller B, Wagner M. 1991 Measurements and stability calculations of the disturbance growth in an unstable three-dimensional boundary layer. Phys. Fluids 3(10):2371-7

[5] Bippes H. 1997 Environmental conditions and transition prediction in 3-D boundary layers. AIAA Paper No.97-1906

[6] Collier, FS. 1993 An overview of recent subsonic laminar flow control flight experiments. AIAA Paper No. 93-2987.

[7] Cumpsty, NA, Head, MR. 1969. The calculation of the three-dimensional turbulent boundary layer. Part III. Comparison of attachment-line calculations with experiment, Aeronautical Quarterly 20, 99.

[8] Dagenhart JR, Saric,WS, Mousseux MC, Stack JP. 1989 Crossflow-vortex instability and transition on a 45-degree swept wing. AIAA Paper No. 89-1892

[9] Dagenhart JR, Saric WS, Mousseux MC. 1990 Experiments on swept-wing boundary layers. Laminar-Turbulent Transition III. Eds. D. Arnal, R. Michel, Springer

[10] Deyhle H, Höhler G, Bippes H. 1993 Experimental investigation of instability wave propagation in a 3-D boundary-layer flow. AIAA J. 31(4):637-45

[11] Deyhle H, Bippes H. 1996 Disturbance growth in an unstable three-dimensional boundary layer and its dependence on initial conditions. J. Fluid Mech. 316:73–113

[12] Gaster M. 1967 On the flow along swept leading edges. Aeronaut. Q. 18:788

[13] Green, JE. 2008 Laminar flow control – back to the future? AIAA Pap. No. 2008-3738.

[14] Hall P, Malik MR, Poll DIA. 1984 On the stability of an infinite swept attachment-line boundary layer. Phil. Trans. Roy. Soc. Lon. A 395:229-45

[15] Haynes TS, Reed HL. 2000 Simulation of swept-wing vortices using nonlinear parabolized stability equations. J. Fluid Mech. 405:325-49

[16] Herbert T. 1997 Parabolized stability equations. Ann. Rev. Fluid Mech. 29:245-83

[17] Janke E, Balakumar P. 2000 On the secondary instability of three-dimensional boundary layers. Theoret. Comput. Fluid Dyn. 14:167–94

[18] Joslin RD. 1998. Aircraft laminar flow control. Ann. Rev. Fluid Mech. 30: 1-29

[19] Kawakami M, Kohama Y, Okutsu M. 1999 Stability characteristics of stationary crossflow vortices in three-dimensional boundary layer. AIAA Pap. No. 99-0811

[20] Kohama Y, Saric WS, Hoos JA. 1991 A high-frequency secondary instability of crossflow vortices that leads to transition. Proc. R.A.S. Boundary Layer Transition and Control Cambridge, UK

[21] Kohama Y, Onodera T, Egami Y. 1996 Design and control of crossflow instability field. Duck PW, Hall, P, eds. 1996 IUTAM Symposium on Nonlinear Instability and Transition in Three-Dimensional Boundary Layers, Amsterdam: Kluwer. 436pp.

[22] Mack LM. 1984 Boundary-layer linear stability theory. AGARD Rpt. 709. Special Course on Stability and Transition of Laminar Flows

[23] Malik MR, Li F, Chang CL. 1994 Crossflow disturbances in three-dimensional boundary layers: Nonlinear development, wave interaction and secondary instability. J. Fluid Mech. 268:1-36

[24] Malik MR, Li F, Chang CL. 1996 Nonlinear crossflow disturbances and secondary instabilities in swept-wing boundary layers. Duck PW, Hall, P, eds. 1996 IUTAM Symposium on Nonlinear Instability and Transition in Three-Dimensional Boundary Layers, Amsterdam: Kluwer. 436pp.

[25] Malik MR, Li F, Choudhari MM, Chang CL. 1999 Secondary instability of crossflow vortices and swept-wing boundary layer transition. J. Fluid Mech. 399:85–115

[26] Pfenninger W. 1965 Some results from the X-21 program. Part I. Flow phenomenon at the leading edge of swept wings. AGARDograph 97

[27] Pfenninger, W., Bacon, J.W. 1969. Amplified laminar boundary layer oscillations and transition at the front attachment line of a 45^{o} swept flat-nosed wing with and without boundary layer suction, Viscous Drag Reduction, C Sinclair Wells, ed., Plenum Press, pp 85-105.

[28] Pfenninger W. 1977 Laminar flow control - Laminarization. AGARD Rpt. 654. Special Course on Drag Reduction

[29] Pfenninger, W, Reed, HL, Dagenhart, JR. 1980 Design considerations of advanced supercritical low drag suction airfoils. Viscous Flow Drag Reduction, AIAA Progress in Astronautics and Aeronautics Series 72.

[30] Poll DIA. 1979 Transition in the infinite swept attachment line boundary layer. Aeronaut. Q. 30: 607

[31] Poll DIA. 1985 Some observations of the transition process on the windward face of a long yawed cylinder. J. Fluid Mech. 150:329-56

[32] Radeztsky RH Jr, Reibert MS, Saric WS, Takagi S. 1993 Effect of micron-sized roughness on transition in swept-wing flows. AIAA Paper No. 93-0076

[33] Reed HL, Saric WS. 1989 Stability of three-dimensional boundary layers. Ann. Rev. Fluid Mech. 21:235

[34] Reed HL, Saric WS, Arnal D. 1996 Linear stability theory applied to boundary layers. Ann. Rev. Fluid Mech. 28:389-428

[35] Reed, HL. 2008 RTO course "Advances in Laminar-Turbulent Transition Modeling", 9-12 June 2008, VKI, Brussels.

[36] Reed, HL, Saric, WS. 2008 Transition mechanisms for transport aircraft. AIAA Pap. No. 2008-3743.

[37] Reibert MS, Saric WS, Carrillo RB Jr, Chapman KL. 1996 Experiments in nonlinear saturation of stationary crossflow vortices in a swept-wing boundary layer. AIAA Paper No. 96-0184

[38] Reshotko E. 1984 Laminar flow control - Viscous simulation. AGARD Rpt. 709. Special Course on Stability and Transition of Laminar Flows

[39] Reshotko E. 1985 Control of boundary-layer transition. AIAA Paper No. 85-0562

[40] Reshotko E. 1994 Boundary layer instability, transition, and control. AIAA Paper No. 94-0001

[41] Reshotko, E. 2008. RTO course "Advances in Laminar-Turbulent Transition Modeling", 9-12 June 2008, VKI, Brussels.

[42] Saric WS, Benmalek A. 1991 Görtler vortices with periodic curvature. Boundary Layer Stability and Transition to Turbulence, FED 114, eds DC Reda, HL Reed, R Kobayashi, ASME, New York:37-42.

[43] Saric WS. 1994 Physical description of boundary-layer transition: Experimental evidence. AGARD Rpt. 793. Progress in Transition Modelling

[44] Saric WS. 1994 Görtler vortices. Ann. Rev. Fluid Mech. 26:379-409

[45] Saric, WS, Carrillo, RB, Reibert, MS. 1998 Leading-edge roughness as a transition control mechanism," AIAA Paper 98-0781.

[46] Saric WS, Reed HL. 2002 Supersonic laminar flow control on swept wings using distributed roughness. AIAA Pap. No. 2002-0147

[47] Saric WS, Reed HL. 2002. Control of transition in supersonic boundary layers: experiments and computations. Keynote Paper, ASME FEDSM-2002-31258, Montreal, July

[48] Saric WS, Reed HL, Kerschen EJ. 2002 Boundary-layer receptivity to freestream disturbances. Ann. Rev. Fluid Mech. 34:291-319

[49] Saric WS, Reed HL, White EB. 2003 Stability and Transition of Three-Dimensional Boundary Layers. Ann. Rev. Fluid Mech. 35:413-40

[50] Saric, WS. 2008. RTO course "Advances in Laminar-Turbulent Transition Modeling", 9-12 June 2008, VKI, Brussels.

[51] Saric WS, Carpenter AL, Reed HL. 2008 Laminar Flow Control Flight Tests for Swept Wings. AIAA Paper No. 2008-3834

[52] von Doenhoff AE, Braslow AL. 1961 The effect of distributed surface roughness on laminar flow. Boundary Layer Control II. Ed. Lachmann, Pergamon: 657-81

[53] Wassermann P, Kloker M. 2002 Mechanisms and control of crossflow-vortex induced transition in a three-dimensional boundary layer. J. Fluid Mech. 456:49-84

[54] White EB, Saric WS. 2005 Secondary instability of crossflow vortices. J. Fluid Mech. 525:275-308

Copyright Statement